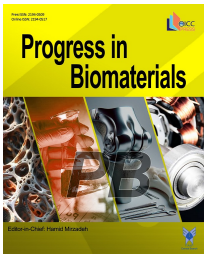

Volume 12, Issue 3, 122316 (1-12)

Progress in Biomaterials (PIBM)

https://doi.org/10.57647/pibm.2023.122316

In vitro Evaluation, Molecular Docking, and Lipinski's Rule Analysis of a new Triazinone-Based Schiff Base for Potential Pharmacological Applications

Akbar Tati[1], Masoumeh Tabatabaee[1,*], Amir Adabi Ardakani[1], Bernhard Neumuller[2]

[1]*Department of Chemistry, Ya.C. Islamic Azad University, Yazd, Iran.*
[2]*Fachbereich Chemie der Universität Marburg, Marburg, Germany.*

[*]**Corresponding author:** mtabatabaee@iau.ir

Original Research

Received:
7 August 2023
Revised:
25 September 2023
Accepted:
28 September 2023
Published online:
30 September 2023

Abstract:

(E)-6-methyl-4-((4-methylbenzylidene)amino)-3-thioxo-3,4-dihydro-1,2,4-triazin-5(2H)-one (**1**), was synthesized from the reaction of 4-amino-3-mercapto-6-methyl-5-oxo-1,2,4-triazine (AMTTO) and 4-methyl benzaldehyde under microwave conditions and characterized through ^{1}H-NMR, FTIR spectroscopy, and single-crystal X-ray diffraction. The Hirshfeld surface was analyzed and results indicate a significant effect of hydrogen interactions and their role in the stability of the crystal lattice of the **1**. The in vitro antibacterial activities were evaluated using the disk diffusion technique. **1** displays moderate to significant effect on bacterial strains. In silico Molecular docking simulations were performed to investigate the interaction **1** with the active site of three target proteins. Discovery Studio Visualizer and LigPlot+ software was used to illustrate molecular docking results. The best confirmation from molecular docking studies shows that the free energies of binding for the studied ligands were −6.7, −6.6, and −6.6 kcal/mol, as were the creation of hydrogen bonds between the studied compound and the target proteins. In silico prediction of physicochemical properties (Lipinski's rule of five) and bioavailability radar were determined by the SwissADME database. The physicochemical property analysis revealed that **1** has a bioavailability score of 0.55. The results of this study indicate that 1 could be a lead compound for developing antimicrobial and antiviral compounds.

Keywords: Thiotriazine Schiff-base compound; Antibacterial Activities; Molecular docking; Lipinski's rules

Cite this article: Tati, A., Tabatabaee, M., Adabi Ardakani, A., Neumuller, B. In vitro Evaluation, Molecular Docking, and Lipinski's Rule Analysis of a new Triazinone-Based Schiff Base for Potential Pharmacological Applications. *Progress in Biomaterials* **12**(3), 1-12 (2023).

1. Introduction

Thiocarbohydrazides are compounds containing N and S atoms, and their derivatives have attracted interest because of the variety of various biological effects (Janowska et al., 2022; Kanso et al., 2021; Greenbaum et al., 2004). Among various thiocarbohydrazide derivatives, 4-amino-3-mercapto-6-methyl-5-oxo-1,2,4-triazine (AMTTO) and 4-amino-5-methyl-2H-1,2,4-triazole-3(4H)-thione (AMTT) are the heterocyclic thiones derived from thiocarbohydrazide that we utilized widely in our studies (Ghassemzadeh et al., 2005b; Bazyari et al., 2021; Ghassemzadeh et al., 2011; Adhamia et al., 2008; Tabatabaee et al., 2009a). The chemical and biochemical interest in thiocarbohydrazide-based compounds is due to the fact that they can coordinate to metals with multi-functional nitrogen or sulfur donor atoms (Ghassemzadeh et al., 2004; Ghassemzadeh et al., 2005a; Adhami et al., 1999; Ghassemzadeh et al., 2014; Ghassemzadeh et al., 2010). For years, Schiff bases have been a significant source of inspiration for chemists and biochemists. Schiff bases are utilized in various fields, including crystal engineering, catalytic reactions, and as photo- or chemo detectors in biological systems (Tsacheva et al., 2023; Sinha et al., 2008; Ceramella et al., 2022; Munawar et al., 2018; Iacopetta et al., 2020; Kumar et al., 2010; Kargar et al., 2021). The main antibacterial activity of Schiff-base compounds is linked to their

capacity to inhibit dihydropteroate synthase (DHPS), an essential enzyme in the bacterial folate biosynthesis pathway. Moreover, Schiff-base ligands frequently contain electron-donating groups and planar conjugated structures, allowing them to chelate metal ions and interact with bacterial membranes or enzymes, which further boosts their antimicrobial effectiveness. This mechanism of action is similar to that of sulfonamide antibiotics, which also target DHPS, suggesting that Schiff-base derivatives could serve as potential frameworks for creating new antibacterial agents (Silver, 2011). In our investigations in the study of the chemistry of AMTTO and AMTT, we have found that they react with aldehydes, which leads to corresponding Schiff-base compounds (Tabatabaee et al., 2006; Tabatabaee et al., 2007), and corresponding Schiff bases are good ligands for coordinating to metal ions (Shirinkam et al., 2014; Ghassemzadeh et al., 2006; Bazyari et al., 2020; Tabatabaee et al., 2009b). In recent years, we have been interested in studying the biological properties of ligands containing S- and N-donor atoms and metal complexes. In this regard, the biological activity of Ag(I) and Cu(I) complexes with AMTT and some sulfonamide compounds have been investigated (Ghaneian et al., 2015; Tahriri et al., 2017). In continuation, in this work, (E)-6-methyl-4-((4-methylbenzylidene)amino)-3-thioxo-3,4-dihydro-1,2,4-triazin-5(2H)-one (1) as a Schiff base compound derived from AMTTO was synthesized, characterized, and molecular docking and Lipinski's rules studies were used to evaluate the biological and antimicrobial properties of the compound.

2. Materials and methods

2.1 General remarks

All purchased chemicals were of reagent grade and used without further purification. 4-amino-6-methyl-3-thioxo-3,4-dihydro-1,2,4-triazin-5(2H)-one was prepared according to literature procedure (Dornow et al., 1964). IR spectra were recorded using FTIR Spectra Bruker Tensor 27 spectrometer (KBr pellets, $4000-400$ cm^{-1}. The elemental analyses were performed using a Costech ECS 4010 CHNS analyzer.

2.2 Synthesis of (E)-6-methyl-4-((4-methylbenzylidene)amino)-3-thioxo-3,4-dihydro-1,2,4-triazin-5(2H)-one (1)

A solution of 4 mmol (0.632 g) AMTTO was mixed with 4-methylbenzaldehyde (0.71 mL, 6 mmol) in a beaker. The beaker was placed in the microwave oven for about 90 s. The reaction mixture was dissolved in methanol (6 mL), the solid residue was filtered and washed with cold ethanol (5 mL), and it was recrystallized from MeOH. Yield: 91%. $C_{12}H_{12}N_4OS$ (260.3): calcd. C 55.32, H 4.61, N 21.51; found: C 55.53, H 4.60, N 21.47. IR (KBr disc, cm^{-1}): N-H 3145, C=O 1694, N=CH (azomethine group) 1605, C=N (triazine) 1565. ^{1}H-NMR (DMSO), δ; ppm: 2.18 (s, 3H, CH_3), 2.34 (s, 3H, CH_3), 7.20-7.87 (4H, Ar), 8.61 (NHimine), 13.71 (NHtriazin).

2.3 Crystal structure analyses of 1

The selected crystal of **1** was covered with a perfluorinated oil and mounted on the tip of a glass capillary under a flow of cold gaseous nitrogen. The orientation matrix and unit cell dimensions were determined from (Stoe IPDS I) reflections (graphite-monochromated Mo-Kα radiation in all cases; $\lambda = 71.073$ pm). The numerical absorption correction was applied for **1**. The structures were solved by the direct methods (SHELXS97) (Sheldrick, 1997) and refined against F^2 by full-matrix least-squares using the program SHELXL-2018 (Sheldrick, 2018). Crystallographic data are listed in Table 1.

2.4 Hirshfeld surface analysis

Hirshfeld surface analysis was employed to explore and quantify intermolecular interactions within the crystal structure of **1**. The surface was generated by importing the Crystallographic Information File (CIF) into CrystalExplorer 17 software (Spackman et al., 2021). As part of the analysis, three-dimensional normalized contact distance (d_{norm}) surfaces were visualized within the range of $0.5-2.0$ Å , displaying red, blue, and white regions. Additionally, two-dimensional fingerprint plots were produced, representing the di and de distances derived from the Hirshfeld surface.

2.5 Evaluation of antibacterial activity by disk diffusion assay

The alcoholic solution of the synthesized compound was tested at a concentration of 500 μg/mL. Two types of Gram-negative bacteria, *Serratia marcescens* (ATCC 13880) and *Escherichia coli* (ATCC 25922), and one type of Gram-positive bacteria, *Staphylococcus aureus* (ATCC 25923), were used to evaluate the antibacterial activity of the prepared Schiff base compound by using the agar disk diffusion assay. In this method, 200 μL of the tested bacterial suspension (108 cells/mL) was inoculated and dispersed on the Mueller Hinton Agar media plate surface. After that, a disk impregnated with 50 μL of 1 was placed on the plate. The cefotaxime antibiotic was used as the positive control for gram-negative bacteria and the novobiocin antibiotic for gram-positive bacteria, whereas 50 μL of 96% ethanol was employed as a negative control. The inhibitory zones were measured in millimeters after the incubation period at 37 °C for 24 h.

2.6 In silico molecular docking study

2.6.1 Receptors crystallographic structures

To computationally identify **1** for antibacterial and antiviral activity, three different drug target proteins were selected as antibacterial targets (Polyisoprenyl-teichoic acid-peptidoglycan teichoic acid transferase TagU (PDB ID 6UF6) from *Bacillus subtilis*, dihydropteroate synthetase (PDB ID 1AJ0) from *Escherichia coli*, and Herpes simplex virus type-1 thymidine kinase (HSV-1 TK) (PDB ID 2KI5) from Herpes simplex virus type-1 was chosen as the antiviral target. The target proteins' crystallographic structures were obtained from the RCSB protein data bank (Protein Data Bank, 2021). The binding pocket was calculated using the Computed

Table 1. Structure refinement data and some geometrical parameters **1**.

Compound	**1**
Instrument	IPDS I (Stoe)
Radiation	Mo-Kα
Formula	$C_{12}H_{12}N_4OS$
M_r	260.31
Color and habit	plates, pale yellow
Crystal system, space group	orthorhombic, $P2_12_12_1$
Crystal dimensions (mm)	$0.45 \times 0.23 \times 0.04$
a (Å)	6.312 (1)
b (Å)	7.807 (1)
c (Å)	25.328 (3)
α (°)	90.00
β (°)	90.00
γ (°)	90.00
V (A^3)	1248.1 (3)
Z	4
D_{calc} (g/cm^3)	1.385
μ (mm^{-1})	0.253
F (000)	544
T	193
Absorption correction	Numerical
h, k, l range	$-7 \leq h \leq 7, -9 \leq k \leq 9, -29 \leq l \leq 31$
Number of measured reflections	7136
Unique reflections (R_{int})	2347 (0.0703)
Reflections with $F_o > 4$ (F_o)	1585
Number of refined parameters	170
Structure solution	direct methods (SHELXS-97)
Refinement against F2	SHELXL-2018
H atoms	calculated positions
R_1	0.0488
wR_2	1123
Goodness-of-fit on F^2	0.890
max. residual electron density	0.20

[a] $w = 1/[\sigma^2(F_o^2) + (0.0452.P)^2]$; $P = [\max(F_o^2, 0) + 2 \cdot F_c^2]/3$

Atlas of the Surface Topography of Proteins (CASTp) and the Supercomputing Facility for Bioinformatics and Computational Biology (SCFBio) server (Computed Atlas of Surface Topography of Proteins (CASTp), 2021, 2022).

2.6.2 Molecular docking simulation

Molecular docking with AutoDock Vina (ADV) was used to determine **1**-receptor pose and affinity of target proteins. The grid box of $40 \times 40 \times 40$ Å with 1 Å spacing for 1AJ0, and 6UF6, and $50 \times 50 \times 50$ Å with 1 Å spacing for 2KI5 were centered on the coordinates of the **1** within the active site of target proteins. Another program setting was considered a default. The molecular docking investigations were performed using Discovery Studio visualizer, and LigPlot$^+$ (Zhang et al., 2022). The compound with the least binding energy (BE) and root mean square deviation (RMSD) was considered the most suitable binding position.

2.7 Physicochemical properties

The SwissADME database (http://www.swissadme.ch/index) was used to predict the physicochemical properties (Lipinski's rule of five) such as molecular weight, number of hydrogen bond acceptors, number of hydrogen bond donors, number of rotatable bonds, octanol–water partition coefficient (cLogP), and topological polar surface area (TPSA) (Varma et al., 2006; Roskoski, 2019). The SMILES line notation was the input data source (Cc1ccc(cc1)/C=N/n1c(=S)[nH]nc(c1=O)C).

3. Results and discussion

Synthesis of (E)-6-methyl-4-((4-methylbenzylidene)amino)-3-thioxo-3,4-dihydro-1,2,4-triazin-5(2H)-one (**1**) under microwave (**1**) irradiation (Scheme 1). **1** was utilized for bioinformatical study to investigate the potential antibacterial and antiviral properties, and physicochemical properties to predict median lethal dose investigations.

The IR spectra of the compound show broad band around at 3145 cm^{-1} which could be related to ν (N-H). It is most probably coupled with stretching frequencies due to the aromatic rings which originally fall in this region. The characteristic band at 1605 cm^{-1} can be assigned as stretching vibration band of the azomethine group (ν (N=CH)). A similar range is also reported in the literature (Tabatabaee et al., 2006). The absorption bands associated to ν (C=O) and ν (C=N) appear at 1694 and 1565 cm^{-1} respectively. ^{1}H-NMR spectra of the compound show methyl groups at 2.18 and 2.34, aromatic hydrogens at 7.20 – 7.87 region and a peak at 13.71 ppm for NH (triazine). Also, a sharp peak (singlet) at $\delta = 8.61$ is observed which can be assigned to the azomethine proton (Tabatabaee et al., 2006).

3.1 Crystal structure of 1

Table 1 shows the crystallographic data of **1**. Selected bond lengths and angles are given in Table 2. **1** crystallizes in the orthorhombic, $P2(1)2(1)2(1)$ space group with four molecules per unit cell. The unit cell parameters are a = 6.312(1) Å, b = 7.807(1) Å, and c = 25.328(3) Å. The basic six-membered ring skeleton in both compounds is planar, while the dihedral angle between the best planes through the triazine ring and the benzole ring is 53° (figure 1). The S1-C1 bond lengths of 1.639(5) Å, O1-C2 of 1.204(5) Å, and the iminic C-N (C5-N) bond distance of 1.278(6) lie in the range observed in similar AMTTO Schiff base compounds Tabatabaee et al., 2006; Tabatabaee et al., 2007. In **1**, some hydrogen bonding links molecules together (N4- H1…N2a: 3.019(4)) Å) and is responsible for building (stacking) an infinite chain along [100] (figure 2).

3.2 Hirshfeld surface calculations

The Hirshfeld surface was computed utilizing the CrystalExplorer software. Figure 3 shows the corresponding fingerprint plots and the mapped Hirshfeld surface analysis of **1**. This research elucidates the intermolecular interactions that dictate the crystal packing of the molecule. In the crystal structure of **1**, H…H interactions constitute the predominant contribution to the Hirshfeld surface, comprising 44.3% of the total surface area. This signifies that van der Waals interactions among hydrogen atoms predominate in the chemical arrangement. The second most significant interactions are H…C/C…H, contributing 15.9%, followed by H…N/N…H at 11.6% and H…S/S…H at 10.9%, indicating the existence of relatively weak hydrogen–heteroatom interactions that stabilize the crystal structure. Additional significant contributions comprise O…C/C…O (4.3%), O…N/N…O (3.0%), and S…C/C…S (3.0%) interactions. Despite being less prominent, these contributions nonetheless influence the overall molecule configuration via dipolar or $\pi - \pi$ interactions. Minor yet discernible interactions encompass S…O/O…S (1.7%), H…O/O…H (1.7%), S…N/N…S (1.5%), and N…C/C…N (1.5%), signifying the existence of weak but significant non-covalent interactions. The C…C interactions provide the smallest contribution of merely 0.6%, suggesting that $\pi - \pi$ stacking interactions between aromatic rings, if existent, are negligible. Table 3 delineates all observed intermolecular interactions and their respective percentage contributions to the Hirshfeld surface. These findings underscore the preeminence of hydrogen-based interactions in crystal packing and offer a thorough comprehension of the supramolecular structure of **1**.

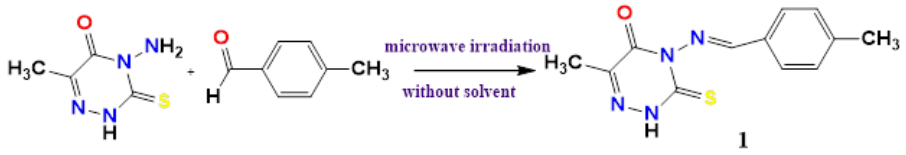

Scheme 1. Synthesis process of **1**.

Table 2. Selected bonds (Å) and angles (°) for **1**.

Bond distances		Bond angles	
S1—C1	1.639(5)	C1—N1—C2	124.4(4)
O1—C2	1.204(5)	C2—N1—N2	119.4(3)
N1—C1	1.366(6)	C5—N2—N1	113.1(4)
N1—N2	1.413(5)	C3—N3—N4	117.0(4)
N2—C5	1.278(6)	C1—N4—N3	127.3(4)
N3—C3	1.289(6)	N4—C1—N1	114.1(4)
N3—N4	1.351(5)	N4—C1—S1	123.3(4)
N4—C1	1.350(5)	N1—C1—S1	122.5(3)

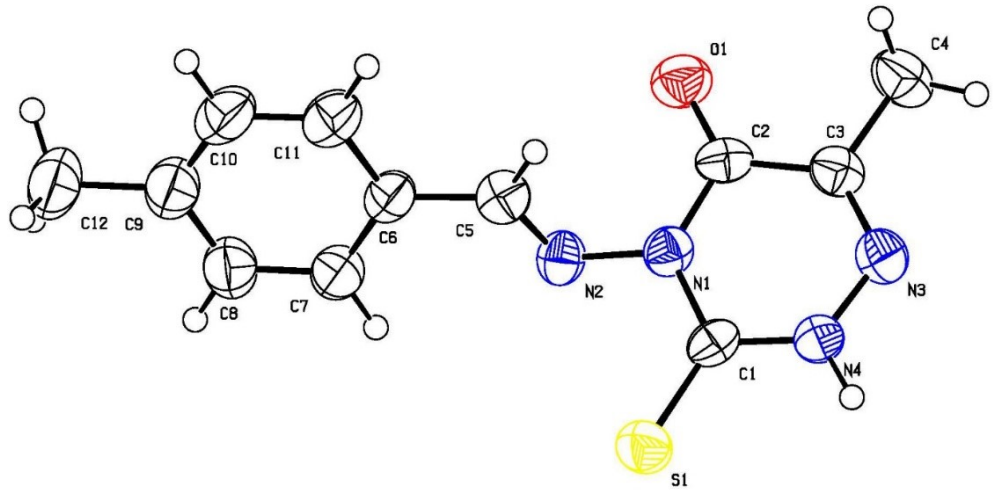

Figure 1. The molecular structure of **1**. Thermal ellipsoids with 50% probability.

3.3 Analysis of antibacterial activity

Based on the CLSI 2021 protocol, the agar disk diffusion method was used to assess the antibacterial activity of the synthesized Schiff base compound at a concentration of 500 μg/mL against *Escherichia coli* (ATCC 25922), *Staphylococcus aureus* (ATCC 25923), and *Serratia marcescens* (ATCC 13880). The results revealed that the compound exhibited varying degrees of antibacterial efficacy depending on the bacterial strain. The highest activity was observed against the Gram-positive bacterium *S. aureus*, with an inhibition zone of 21 ± 2 mm, which is comparable to the standard antibiotic novobiocin (28 ± 2 mm), indicating strong

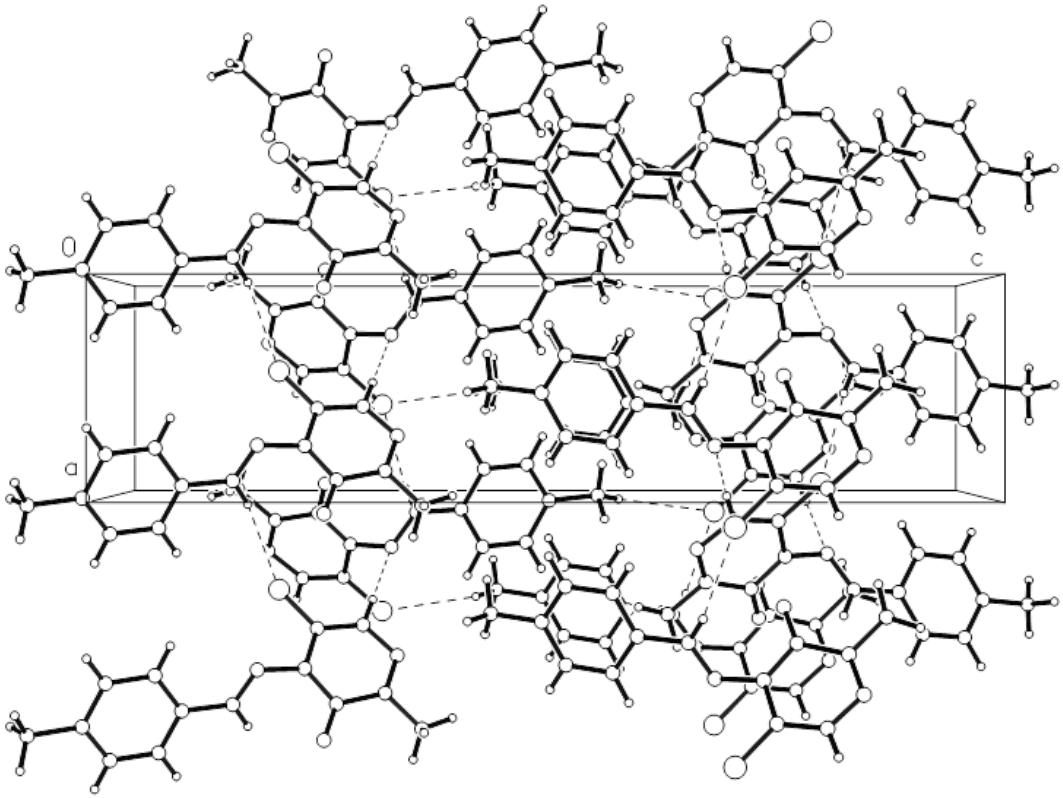

Figure 2. Perspective view of the crystal structure of **1**. Molecules are stacked in an infinite chain along [100].

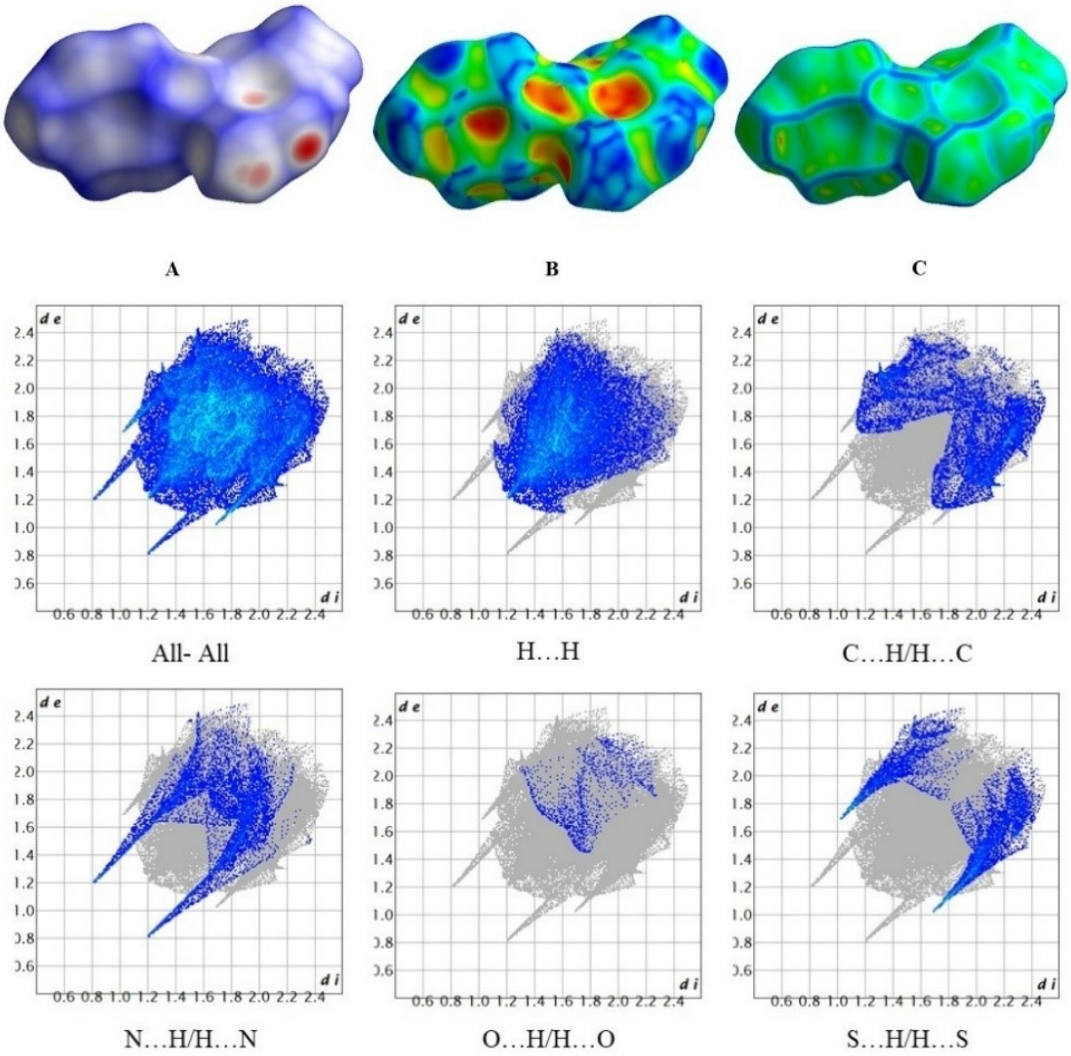

Figure 3. (a) Hirshfeld surfaces of **1** (A) dnorm, (B) shape index and (C) curvedness. (b) Fingerprint plots of **1**.

antibacterial potential (Table 4). Against *S. marcescens*, a Gram-negative strain, the compound showed moderate activity with an inhibition zone of 19 ± 1 mm, whereas the activity against *E. coli* was relatively weak, with a zone of 11 ± 1 mm. In all cases, the inhibition zones produced by the compound were significantly larger than those of the negative control (96% ethanol), confirming that the observed antibacterial effects were attributable to the compound itself (figure 4). These findings suggest that the Schiff base compound is more effective against Gram-positive bacteria, likely due to structural differences in the bacterial cell wall that facilitate greater permeability.

The antibacterial activity of numerous Schiff-base compounds has been extensively reported in the literature. For comparative purposes, the antibacterial activity of compound **1** is evaluated with some selected Schiff bases, as summarized in Table 5, based on their inhibition zone diameters (IZD). As shown in Table 5, compound **1** exhibits greater antibacterial activity against *Staphylococcus aureus* compared to the other Schiff-base compounds. Its activity against *Escherichia coli* is also comparable to that of the other compounds listed.

3.4 Molecular docking simulation

The docking conformation of **1** in the active site of dihydropteroate synthetase from *Escherichia coli* (PDB ID: 1AJ0) in the best conformation with 0.92 RMSD, and the value of the free binding energy was −6.7 kcal/mol, showing that this compound formed three hydrogen bonds with active site residues Asn22 and Thr62. Similarly, the docking conformation of **1** in the active site of the Polyisoprenyl-teichoic acid-peptidoglycan teichoic acid transferase TagU (PDB ID: 6UF6) from *Bacillus subtilis* in the best conformation with 0.82 RMSD, and the value of the free binding energy was −6.6 kcal/mol, and showed that this compound formed two hydrogen bonds with active site residues Ile71, Gly73, Val149, and Val151. The docking conformation of **1** in the active site of HSV-1 thymidine kinase (2KI5) from Herpes Simplex Virus type **1** in the best conformation with 0.67 RMSD, and the value of the free binding energy was −6.6 kcal/mol, and it showed that this compound formed one hydrogen bond with active site residue, Gly92. The docking score for target proteins is shown in Table 6. The 2D interaction by the analysis of compound-receptor using LigPlot^{+} is shown in figure 5, and the 3D docking inter-

Table 3. Intermolecular contacts and their percentage distribution.

Intermolecular contacts	Percentage distribution
H…H	44.3%
C…C	0.6%
H…O/O…H	1.7%
H…C/C…H	15.9%
H…N/N…H	11.6%
H…S/S…H	10.9%
N…C/C…N	1.5%
O…C/C…O	4.3%
O…N/N…O	3%
S…O/O…S	1.7%
S…N/N…S	1.5%
S…C/C…S	3%

Table 4. Antibacterial activities of 1 tested by disk diffusion method.

Bacterial name	Diameter of zone of inhibition (mm)			
	1	Ethanol	Cefotaxime	Novobiocin
Serratia marcescens	19 ± 1	6 ± 1	30 ± 2	-
Escherichia coli	11 ± 1	6 ± 1	30 ± 2	-
Staphylococcus aureus	21 ± 2	5 ± 1	-	28 ± 2

action simulation is shown by utilizing Discovery Studio visualizer in figure 6.

3.5 Lipinski's rule

The bioavailability radar offers a visual representation of the critical physicochemical parameters that affect the oral availability of bioactive compounds. **1** demonstrated a bioavailability score of 0.55 in this investigation (Table 7). **1** meets all but one of the parameters outlined in Lipinski's Rule of Five (RO5), which identifies the important molecular characteristics that are associated with favorable oral drug absorption. It is important to note that the INSATU value of 0.17 marginally deviates from the optimal threshold (> 0.25), suggesting a relatively low degree of saturation (figure 7). The other physicochemical parameters of **1** are within the favorable range for drug-likeness. The molecular weight of 260.31 g/mol is significantly lower than the 500 g/mol threshold. The balanced hydrophilic-lipophilic pro-

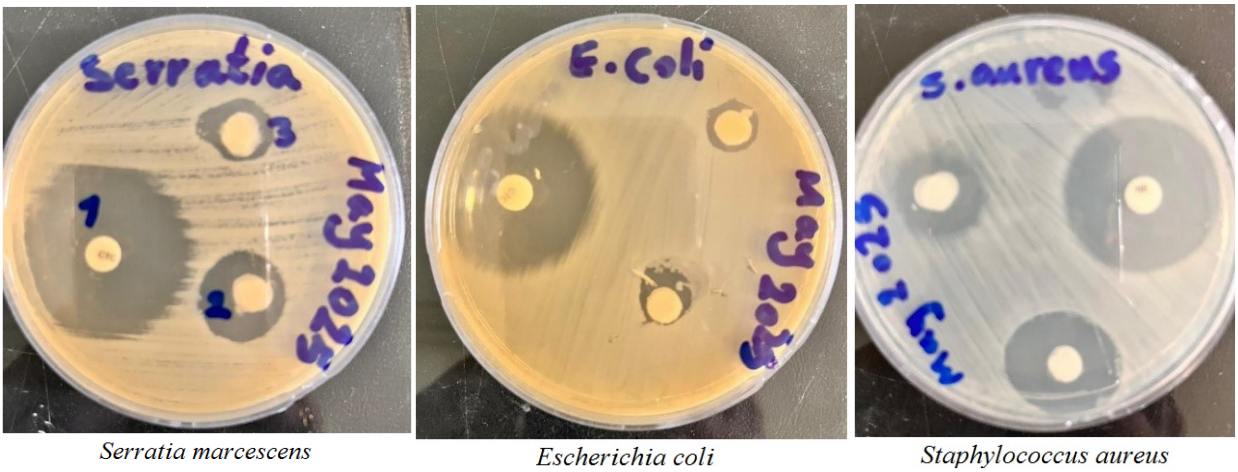

Serratia marcescens *Escherichia coli* *Staphylococcus aureus*

Figure 4. Results of evaluation of antibacterial activity of **1**.

Table 5. Comparison of the antibacterial activity of compound **1** with selected Schiff-base compounds.

Structure	Antimicrobial activity	Ref.
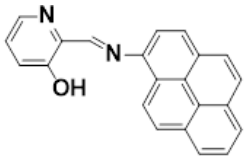	IZD = 14 mm (*E. coli*)	16
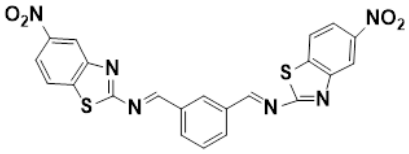	IZD = 14 mm (*S. aureus*)	16
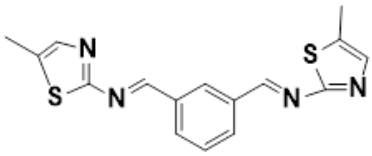	IZD = 10 mm (*S. aureus*)	16
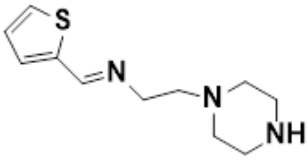	IZD = 12 mm (*S. aureus*)	16
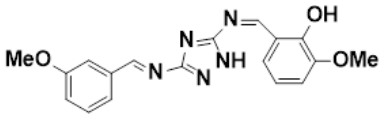	IZD = 13 mm (*E. coli*)	16
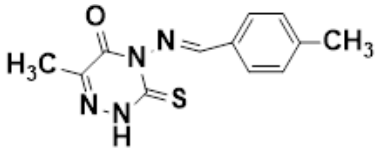	IZD = 11 mm (*E. coli*) IZD = 21 mm (*S. aureus*)	Schiff-base in this study:

Table 6. The docking score for target proteins.

Target proteins (PDB ID)	Binding energy (kcal/mol)	RMSD	Amino acids residues
1AJ0	−6.7	0.92	Asn22, Thr62
6UF6	−6.6	0.82	Ile71, Gly73, Val149, Val151
2KI5	−6.6	0.67	Gly92

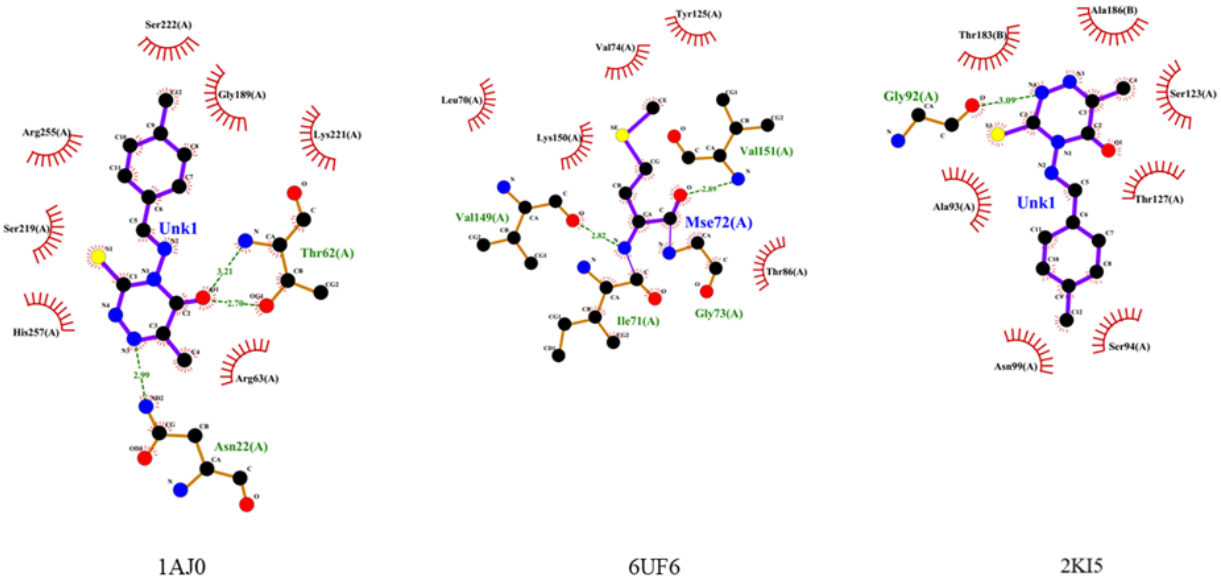

Figure 5. The 2D structure of compound-receptor interaction was made by LogPlot^{+} (Carbon atoms are shown in black, oxygen in red, nitrogen in blue, and sulfur in yellow).

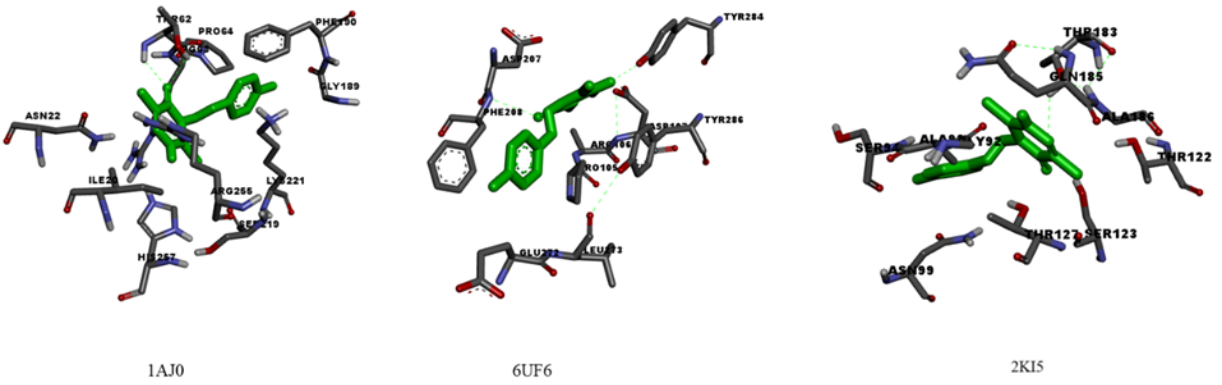

Figure 6. Protein targets active site complexed with 1 was made using the Discovery Studio visualizer.

file, as indicated by the calculated Log P (cLogP) of 2.27 and XLOGP3 of 1.86, is advantageous for membrane permeability without compromising solubility. The optimal range (< 140 Å^2) is occupied by the topological polar surface area (TPSA) of 95.13 Å^2, which enables sufficient gastrointestinal absorption. **1** is composed of one hydrogen-bond donor (HBD) and three hydrogen-bond acceptors (HBA), which are within the limits established by RO5 (≤ 5 and ≤ 10, respectively). Furthermore, the compound possesses two rotatable bonds, which suggests a low level of molecular flexibility. This property is associated with improved oral bioavailability and membrane permeability. The predicted solubility class is soluble, and the gastrointestinal absorption is considered to be high. **1** is also compliant with RO5 filters and satisfies the criteria for lead-likeness, indicating that it could be a promising launching point for drug development (Lipinski et al., 2001; Hughes et al., 2008). The overall bioavailability profile of **1** is favorable, which reinforces its potential as a viable oral drug candidate, despite the minor deviation in saturation (INSATU).

4. Conclusion

A Schiff-base compound, (E)-6-methyl-4-((4-methylbenzylidene)amino)-3-thioxo-3,4-dihydro-1,2,4-triazin-5(2H)-one was synthesized and characterized through ^{1}H-NMR, FTIR spectroscopy, and X-ray diffraction techniques. The Hirshfeld surface was evaluated, and both 2D fingerprint plots and 3D illustrations were obtained from the Hirshfeld surface analysis. The results indicate a significant effect of hydrogen interactions and their role in the stability of the crystal lattice of the **1** compound. The antibacterial results showed that **1** displays moderate to significant effect on bacterial strains (inhibition zones of $11-21$ mm). In silico Molecular docking simulations were performed using AutoDock Vina software to investigate the interaction **1** with the active site of three target proteins (PDB ID: 1AJ0, 6UF6, and 2KI5). In silico prediction of physicochemical properties and bioavailability radar were determined by the SwissADME database. Overall, **1** satisfies essential drug-likeness requirements, including adherence to the Rule of Five, adequate solubility, and advantageous bioavailability metrics, suggesting its potential as a viable oral phar-

Table 7. Molecular properties of 1 according to Lipinski's rules.

Parameter	Results
Formula	$C_{12}H_{12}N_4OS$
Molecular Weight (g/mol)	260.31
Octanol–water partition coefficient (c log P)	2.27
Number of hydrogen-bond donors (HBD)	1
Number of hydrogen-bond acceptors (HBA)	3
Number of rotatable bonds (FLEX)	2
Topological Polar Surface Area (A^2)	95.13
XLOGP3	1.86
Log S	−3.86
INSATU	0.17
Solubility class	Soluble
Gastrointestinal absorption	High
Leadlikeness	Yes
Pfizer's rule of five or simply the rule of five (RO5)	Yes
Bioavailability score	0.55

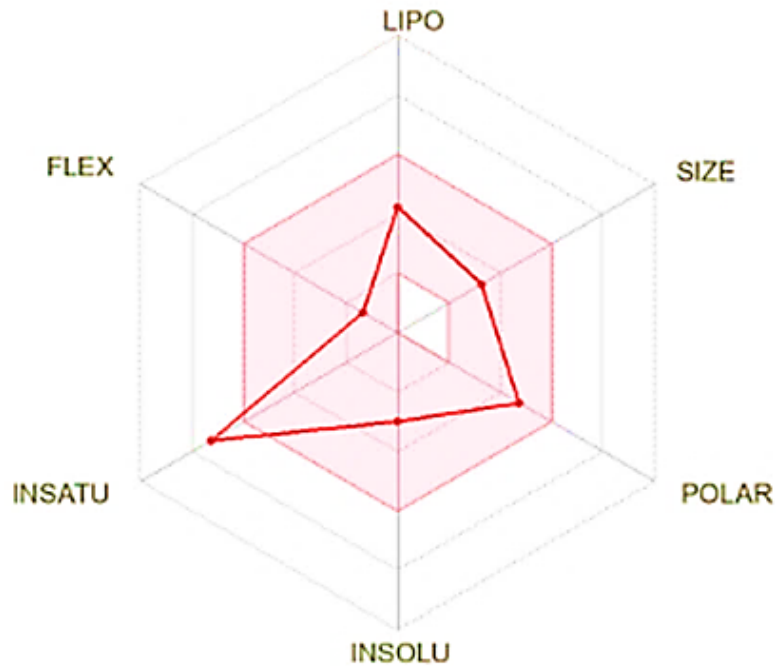

Figure 7. Bioavailability radar of the tested compound.

maceutical option. The results of this study indicate that (E)-6-methyl-4-((4-methylbenzylidene)amino)-3-thioxo-3,4-dihydro-1,2,4-triazin-5(2H)-one could be a lead compound for developing antimicrobial and antiviral compounds.

Acknowledgment
The authors are grateful to Yazd Branch, Islamic Azad University, for the support of this work.

Supplementary material
CCDC 2414832 contains the supplementary crystallographic data for **1**. These data can be obtained free of charge via www.ccdc.cam.ac.uk/conts/retrieving.html [or from the Cambridge Crystallographic Data Centre (CCDC), 12 Union Road, Cambridge CB2 1EZ, UK; fax: +44(0)1223-336033; email: deposit@ccdc.cam.ac.uk]. Structure factors are available from the authors.

Authors contributions
Authors have contributed equally in preparing and writing the manuscript.

Availability of data and materials
The data that support the findings of this study are available from the corresponding author, upon reasonable request.

Conflict of interests
The authors declare that they have no known competing financial interests or personal relationships that could have appeared to influence the work reported in this paper.

References

Adhami F., Ghassemzadeh M., Heravi M. M., Taeb A., Neumüller B. (1999) "Synthesis and Crystal Structure of a New Silver(I) Complex" *Z. Anorg. Allg. Chem.* **625**:1411–1412. DOI: https://doi.org/10.1002/(SICI)1521-3749(199909)625:9¡1411.

Adhamia F., Tabatabaee M., Gassemzadehc M., Neumüllerd B. (2008) "A New Complex as a Dimer of a Silver ion with AMTTO and Phosphane Ligands. The Crystal Structure of {[(AMTTO)Ag(PPh3)2]NO3}2.0.5CH3OH.0.5H2O" *Z. Anorg. Allg. Chem.* **634**:1466–1468. DOI: https://doi.org/10.1002/zaac.200800072.

Bazyari P., Tabatabaee M., Nasirizadeh N., Dušek M., Eigner V. (2021) "A Unique Example of a Co crystal of $[Co(AMTTO)_2(H_2O)_2](NO_3)_2$ and $[Co(AMTTO)_2(CH_3CN)_2](NO_3)_2$ AMTTO=4 amino 5 methyl 1,2,4 triazol 3(2H) thione)" *J. Chem. Crystal.* **51**:574–581. DOI: https://doi.org/10.1007/s10870-021-00882-5.

——— (2020) "Crystal and Molecular Structures of Mononuclear Coordinated Copper(I) Complexes with Thio-triazole and Thio-triazine based Schiff base Ligands" *Z. Anorg. Allg. Chem.* **646**:1444–1448. DOI: https://doi.org/10.1002/zaac.202000191.

Ceramella J., Escopeta D., Catalano A., Cirillo F., Lappano R., Sinicropi M. S. (2022) "A Review on the Antimicrobial Activity of Schiff Bases: Data Collection and Recent Studies" *Antibiotics* **11**:191. DOI: https://doi.org/10.3390/antibiotics11020191.

Computed Atlas of Surface Topography of Proteins (CASTp) (2021), http://sts.bioe.uic.edu/castp/index.html?1aj0.

——— (2022), http://www.scfbio-iitd.res.in/

Dornow A., Menzel H., Marx P. (1964) "Synthesenstickstoffhaltiger Heterocyclen, XXVII. & UUML;ber 1.2. 4-Triazine, I Darstellungeinigerneuer s-Triazolo [3.2-c]-as- triazine" *Chem. Ber.* **97**:2173–2175. DOI: https://doi.org/10.1002/cber.19640970811.

Ghaneian M. T., Tabatabaee M., Ehrampoush M. H., Jebali A., Hekmatimoghaddam S. H., Fallahzadeh H., Fallahzadeh R. A. (2015) "Synthesis of Ag(I) and Cu(I) Complexes With 4-Amino-5-Methyl-2h-1,2,4-Triazole-3(4h)-Thione Ligand as Thiocarbohydrazide Derivatives and Their Antimicrobial Activity, Pharm" *Chem. J.* **49**:210–231. DOI: https://doi.org/10.1007/s11094-015-1258-0.

Ghassemzadeh M., Bahemmat S., Mahmoodabadi M., Rezaii-Rad B., Monfared H. H., Mottefakeri E., Neumüller B. (2010) "New mono- and binuclear Pd(II) complexes containing 1,2,4-triazole moieties" *Polyhedron* **29**:3036–3045. DOI: https://doi.org/10.1016/j.poly.2010.08.012.

Ghassemzadeh M., Bahemmat S., Tabatabaee M., Nassiri S., Neumüller B. (2011) "Synthesis, characterization and crystal structures of palladium(II) complexes containing neutral, one and twofold deprotonated 1,2,4-triazine species" *Polyhedron* **30**:1760–1766. DOI: https://doi.org/10.1016/j.poly.2011.03.048.

Ghassemzadeh M., Firouzi R., Shirkhani S., Amiri S. R., Neumüller B. (2014) "New dinuclear copper(I) metallacycles containing bis-Schiff base ligands fused with two 1,2,4-triazole rings: Synthesis, characterization, molecular structures and theoretical calculations" *Polyhedron* **69**:188–196. DOI: https://doi.org/10.1016/j.poly.2013.11.030.

Ghassemzadeh M., Mirza-Aghayan M., Neumüller B. (2005a) "Syntheses and characterization of the first platinum complex and new palladacycles of N,S-chelating agent in "triplex" form: molecular structures of [(AMTTO)PtCl2]3 Æ 4.5THF and [(AMTTO)PdX2]3 Æ 8MeOH (X = Cl and Br) (AMTTO=4-amino-6-methyl-1,2,4-triazine-3-thione-5-one) " *Inorg. Chim. Acta* **358**:2057–2065. DOI: https://doi.org/10.1016/j.ica.2004.12.025.

Ghassemzadeh M., Pooramini M. M., Tabatabaee M., Heravi M. M., Neumüller B. (2004) "Syntheses, Characterization and X-Ray Structures of the first Copper(I) and Silver(I) Complexes with ATT (ATT 6-Aza-2-thiothymine) " *Z. Anorg. Allg. Chem.* **630**:403–406. DOI: https://doi.org/10.1002/zaac.200300362.

Ghassemzadeh M., Tabatabaee M., Mirrokni Z., Neumüller B. (2005b) "Synthesis, Characterization and Crystal Structure of Dimeric $\{[(AMTTO)_2Ag]NO_{32}$ (AMTTO 4-Amino-6-methyl-1,2,4-triazine-3(2H)-thione-5-one)$\}$" *Z. Anorg. Allg. Chem.* **631**:832–834. DOI: https://doi.org/10.1002/zaac.200500012.

Ghassemzadeh M., Tabatabaee M., Pooramini M. M., Heravi M. M., Eslami A., Neumüller B. (2006) "Synthesis, Characterization of a Novel 1,2,4-Thiotriazine Derivative (CAMTTO), and Copper(I) and Silver(I) Complexes thereof (CAMTTO {(4-[(4-Chlorobenzylidene)-amino]-6-methyl-3-thioxo-[1,2,4]- triazin-3,4-dihydro(2H)-5-one)} " *Z. Anorg. Allg. Chem.* **632**:786–792. DOI: https://doi.org/10.1002/zaac.200500334.

Greenbaum D. C., Mackey Z., Hansell E., Doyle P., J.Gut, Caffrey C. R., Lehrman J., Rosenthal P. J., J. H. McKerrow, Chibale K. (2004) "Synthesis and Structure-Activity Relationships of Parasiticidal Thiosemicarbazone Cysteine Protease Inhibitors against Plasmodium falciparum, Trypanosoma brucei, and Trypanosoma cruzi" *J. Med. Chem.* **47**:3212–3219. DOI: https://doi.org/10.1021/jm030549j.

Hughes J. D., Blagg J., Price D. A., Bailey S., Decrescenzo G. A., Devraj R. V., Weidolf L. (2008) "Physiochemical drug properties associated with in vivo toxicological outcomes" *Bioorg. Med. Chem. Lett.* **10**:367–373. DOI: https://doi.org/10.1016/j.bmcl.2008.07.086.

Iacopetta D., Lappano R., Mariconda A., Ceramella J., Sinicropi S. M., Saturnino C., Talia M., et al. (2020) "Newly synthesized imino-derivatives analogues of resveratrol exert inhibitory effects in breast tumor cells " *Int. J. Mol. Sci.* **21**:7797. DOI: https://doi.org/10.3390/ijms21207797.

Janowska S., Khylyuk D., Andrzejczuk S., Wujec M. (2022) "Design, Synthesis, Antibacterial Evaluations and In Silico Studies of Novel Thiosemicarbazides and 1,3,4-Thiadiazoles" *Molecules* **27**:3161. DOI: https://doi.org/10.3390/molecules27103161.

Kanso F., Khalil A., Noureddine H., El-Makhour Y. (2021) "Therapeutic perspective of thiosemicarbazones derivatives in inflammatory pathologies: A summary of in vitro/in vivo studies" *International Immunopharmacology* **96**:107778. DOI: https://doi.org/10.1016/j.intimp.2021.107778.

Kargar H., Fallah-Mehrjardi M., Ashfaq M., Munawar K., Tahir M. N., Behjatmanesh-Ardakani R., Rudbari H. A., Adabi Ardakani A., Sedighi-Khavidak S. (2021) "Zn(II) complexes containing O,N,N,O-donor Schiff base ligands: synthesis, crystal structures, spectral investigations, biological activities, theoretical calculations and substitution effect on structures" *J. Coord. Chem.* **74**:2720–2740. DOI: https://doi.org/10.1080/00958972.2021.1990271.

Kumar K. S., Ganguly S., Veerasamy R., De Clercq E. (2010) "Synthesis, antiviral activity and cytotoxicity evaluation of Schiff bases of some 2-phenyl quinazoline-4 (3) H-ones" *Eur. J. Med. Chem.* **45** (5474–5479) DOI: https://doi.org/10.1016/j.ejmech.2010.07.058.

Lipinski C. A., Lombardo F., Dominy B. W., Feeney P. J. (2001) "Experimental and computational approaches to estimate solubility and permeability in drug discovery and development settings" *Adv. Drug Deliv. Rev.* **46**:3–26. DOI: https://doi.org/10.1016/S0169-409X(00)00129-0.

Munawar K. S., Haroon S. M., Hussain S. A., Raza H. (2018) "Schiff bases: Multipurpose pharmacophores with extensive biological applications" *J. Basic Appl. Sci.* **14**:217–229.

Protein Data Bank (2021), https://www.rcsb.org

Roskoski R. (2019) "Properties of FDA-approved small molecule protein kinase inhibitors" *Pharmacological Research* **144**:19–50. DOI: https://doi.org/10.1016/j.phrs.2019.03.006.

Sheldrick G. M. (2018) "SHELXL-2018 Program for Crystal Structure Refinement. University of Göttingen "

——— (1997) "SHELXL-97, Program for Crystal Structure Solution and Refinement Göttingen"

Shirinkam B., Tabatabaee M., Kukovec B.-M., Oliver C.L., Ghassemzadeh M. (2014) "Preparation, spectroscopic characterization, and crystal structure of a mixed-ligand silver(I) complex with 1,2,4-triazole-based Schiff base and triphenylphosphine" *Monatsh. Chem.* **145**:1753–1757. DOI: https://doi.org/10.1007/s00706-014-1256-z.

Silver L. L. (2011) "Challenges of Antibacterial Discovery" *Clin Microbiol Rev.,* DOI: https://doi.org/10.1128/cmr.00030-10.

Sinha D., Tiwari A. K., Singh S., Shukla G., Mishra P., Chandra H., Mishra A. K. (2008) "Synthesis, characterization and biological activity of Schiff base analogues of indole-3-carboxaldehyde" *Eur. J. Med. Chem.* **43**:160–165. DOI: https://doi.org/10.1016/j.ejmech.2007.03.022.

Spackman P. R., Turner M. J., McKinnon J. J., Wolff S. K., Grimwood D. J., Jayatilaka D., Spackman M. A. (2021) "Crystal Explorer: a program for Hirshfeld surface analysis, visualization and quantitative analysis of molecular crystals" *J. Appl. Cryst.* **54**:1006–1011. DOI: https://doi.org/10.1107/S1600576721002910.

Tabatabaee M., Ghassemzadeh M., Neumüller B. (2009a) "Syntheses, Characterization and X-ray Structure of the First Silver(I) Complexes with 4-Amino-3-thioxo-3,4-dihydro-1,2,4-triazin-5(2H)-one" *Z. Anorg. Allg. Chem.* **635**:1620–1625. DOI: https://doi.org/10.1002/zaac.200801417.

Tabatabaee M., Ghassemzadeh M., Sadeghi A., Shahriary M., Neumüller B. (2009b) "A. Rothenberger, Synthesis, Characterization and X-ray Structures of AMTT-Type Schiff bases and two Cu^{I} Complexes (AMTT 4-amino-5-methyl-2H-1,2,4-triazole-3(4H)-thione) " *Z. Anorg. Allg. Chem.* **635**:120–124. DOI: https://doi.org/10.1002/zaac.200800366.

Tabatabaee M., Ghassemzadeh M., Zarabi B., Heravi M. M., Anary-Abbasinejad M., Neumüller B. (2007) "Solvent-Free Microwave Synthesis of (Aryland Heteroaryl-methylene)-amino Derivatives of 4-Amino-6-methyl-5-oxo-3-thioxo-2H-1,2,4-triazine and 4-Amino-5-methyl-3-thioxo-2H-1,2,4-triazole: Crystal Structure of 6-Methyl-4-(3-nitrobenzylideneamino)- 5-oxo-3-thioxo-2H-1,2,4-triazine Phosphorus Sulfur Silicon " *Relat. Elem.* **182**:677–686. DOI: https://doi.org/10.1080/10426500601047461.

Tabatabaee M., Ghassemzadeh M., Zarabi B., Neumüller B. (2006) "Synthesis and Crystal Structure of Schiff Bases Based on AMTTO (AMTTO = 4-Amino-6-methyl-3-thio-3,4-dihydro-1,2,4-triazin5(2H)-one)" *Z. Naturforsch* **61**:1421–1425. DOI: https://doi.org/10.1515/znb-2006-1116.

Tahriri M., Yousefi M., Mehrani K., Tabatabaee M., Dehghani Ashkezari M. (2017) "Synthesis, Characterization and Antimicrobial Activity of Two Novel Sulfonamide Schiff, Base Compounds" *Pharm. Chem. J.* **51**:425–438. DOI: https://doi.org/10.1007/s11094-017-1626-z.

Tsacheva I., Todorova Z., Momekova D., Momekov G., Koseva N. (2023) "Pharmacological Activities of Schiff Bases and Their Derivatives with Low and High Molecular Phosphonates" *Pharmaceuticals* **16**:938. DOI: https://doi.org/10.3390/ph16070938.

Varma M. V., Perumal O. P., Panchagnula R. (2006) Functional role of P-glycoprotein in limiting peroral drug absorption: optimizing drug delivery *"Curr. Opin. Chem. Biol.",* DOI: https://doi.org/10.1016/j.cbpa.2006.06.015.

Zhang A., Li W., Liu X., Wu M., Xuan G. (2022) "Biological Evaluation and in Silico Studies of Several Substituted Benzene Sulfonamides as Potential Antibacterial Agents" *Journal of Physics* DOI: https://doi.org/10.1088/1742-6596/1624/2/022058.